Molecular Biology of the Cell
Vol. 20, 389–399, January 1, 2009

# Molecular Clustering of STIM1 with Orai1/CRACM1 at the Plasma Membrane Depends Dynamically on Depletion of $Ca^{2+}$ Stores and on Electrostatic Interactions

**Nathaniel Calloway,* Monika Vig,† Jean-Pierre Kinet,† David Holowka,* and Barbara Baird***

*Department of Chemistry and Chemical Biology, Cornell University, Ithaca, NY 14850; and †Beth Israel-Deaconess Medical Center, Harvard Medical School, Boston, MA 02215

Submitted November 12, 2007; Revised September 12, 2008; Accepted October 29, 2008
Monitoring Editor: Jennifer Lippincott-Schwartz

**Activation of store operated $Ca^{2+}$ entry involves stromal interaction molecule 1 (STIM1), localized to the endoplasmic reticulum (ER), and calcium channel subunit (Orai1/CRACM1), localized to the plasma membrane. Confocal microscopy shows that thapsigargin-mediated depletion of ER $Ca^{2+}$ stores in RBL mast cells causes a redistribution of STIM1, labeled with monomeric red fluorescent protein (mRFP), to micrometer-scale ER-plasma membrane junctions that contain Orai1/CRACM1, labeled with monomeric *Aequorea coerulescens* green fluorescent protein (AcGFP). Using fluorescence resonance energy transfer (FRET), we determine that this visualized coredistribution is accompanied by nanoscale interaction of STIM1-mRFP and AcGFP-Orai1/CRACM1. We find that antigen stimulation of immunoglobulin E receptors causes much less Orai1/CRACM1 and STIM1 association, but strong interaction is observed under conditions that prevent refilling of ER stores. Stimulated association monitored by FRET is inhibited by sphingosine derivatives in parallel with inhibition of $Ca^{2+}$ influx. Similar structural and functional effects are caused by mutation of acidic residues in the cytoplasmic segment of Orai1/CRACM1, suggesting a role for electrostatic interactions via these residues in the coupling of Orai1/CRACM1 to STIM1. Our results reveal dynamic molecular interactions between STIM1 and Orai1/CRACM1 that depend quantitatively on electrostatic interactions and on the extent of store depletion.**

## INTRODUCTION

Modulation of cytosolic $Ca^{2+}$ levels is central to the regulation of a wide range of physiological processes. One of the key mechanisms of $Ca^{2+}$ regulation in mammalian cells is calcium release-activated calcium (CRAC) influx, in which the depletion of intracellular stores of $Ca^{2+}$ triggers a sustained influx of $Ca^{2+}$ from the extracellular medium. The CRAC current ($I_{CRAC}$) was characterized initially in hematopoietic cells in electrophysiological studies (Lewis and Cahalan, 1989; Hoth and Penner, 1992), but the proteins that mediate this process eluded investigators for nearly 20 y.

Recent advances are identification of two key proteins that regulate $I_{CRAC}$: stromal interaction molecule 1 (STIM1) that localizes to the endoplasmic reticulum (ER) and Orai1/CRACM1 that is found in the plasma membrane. Expression of these two proteins is sufficient to reconstitute $I_{CRAC}$ in deficient cells (Soboloff *et al*., 2006). STIM1 has a $Ca^{2+}$ binding, EF-hand domain positioned in the ER lumin (Roos *et al*., 2005; Liou *et al*., 2005). Orai1/CRACM1 has been identified as the CRAC channel in the plasma membrane (Feske *et al*., 2006, Vig *et al*., 2006a). Both STIM1 (Baba *et al*., 2008) and Orai1/CRACM1 (Vig *et al*., 2008) have recently been shown to be essential for stimulated mast cell degranulation. These discoveries have opened up a pathway to mechanistic understanding of $I_{CRAC}$ and, in particular, the participation of these two proteins.

In initial studies, treatment of cells with the sarcoplasmic/endoplasmic reticulum calcium ATPase (SERCA) inhibitor thapsigargin were shown to cause redistribution of STIM1 to form punctae at or near the plasma membrane, and these were identified as locations of CRAC activity (Liou *et al*., 2005; Luik *et al*., 2006). Mutations in the EF-hand domain of STIM1 resulted in constitutively active $I_{CRAC}$ and translocation of STIM1 to the plasma membrane, indicating that this protein is the $Ca^{2+}$ sensor responsible for transmitting the signal for store-operated calcium entry (SOCE) (Liou *et al*., 2005). These results imply that these punctae are regions where ER and plasma membranes become closely associated, such that STIM1 can relay the signal that stores are empty to Orai1/CRACM1. This visualization by microscopy provides evidence that functionally relevant STIM1-Orai1/CRACM1 association occurs on the micrometer scale, but it cannot specify whether direct interactions between these two proteins are involved in this activation mechanism. Two recent studies demonstrated nanoscale interactions between STIM1 and Orai1/CRACM1 as detected with fluorescence resonance energy transfer (FRET) in human embryonic kid-

This article was published online ahead of print in *MBC in Press* (http://www.molbiolcell.org/cgi/doi/10.1091/mbc.E07–11–1132) on November 5, 2008.

Address correspondence to: Barbara Baird (bab13@cornell.edu).

Abbreviations used: AcGFP, *Aequorea coerulescens* green fluorescent protein; CRAC, calcium release-activated calcium; CRACM1, CRAC messenger 1 (also called Orai1); DMS, *N*,*N*′-dimethylsphingosine; FRET, fluorescence resonance energy transfer; $I_{CRAC}$, calcium release-activated calcium current; mRFP, monomeric red fluorescent protein; PH, pleckstrin homology (domain); SERCA, sarcoplasmic/endoplasmic reticulum calcium ATPase; SOC, Store operated $Ca^{2+}$; STIM1, stromal interaction molecule 1; TMS, *N*,*N*,*N*-trimethylsphingosine.

ney (HEK) cells (Muik *et al*., 2008) and in T cells (Barr *et al*., 2008).

The present study shows that interactions between STIM1 and Orai1/CRACM1 occur in a highly regulated manner when SOCE is activated by IgE receptor stimulation of RBL mast cells. To understand this regulation, we compared, with confocal imaging and FRET, the antigen-stimulated association of STIM1 and Orai1/CRACM1 under conditions where the extent of store refilling is altered by elimination of extracellular $Ca^{2+}$ and by treatment with $Gd^{3+}$, which inhibits SOCE. Our results reveal that molecular interaction between STIM1 and Orai1/CRACM1 depends dynamically on the extent of store depletion. Furthermore, inhibition of this interaction by sphingosine derivatives and by point mutations of acidic residues in Orai1/CRACM1 suggest an electrostatic mechanism involving the C-terminal segment of Orai1/CRACM1, providing new insight into the mechanism of antigen-mediated activation and regulation of $I_{CRAC}$.

## MATERIALS AND METHODS

### *Cloning and Constructs*

STIM1 cDNA was encoded in a pcDNA4-myc-his vector (Vig *et al*., 2006b). The fusion of monomeric red fluorescent protein (mRFP) to the 3′ end of STIM1 was constructed by cloning mRFP cDNA from mRFP-pRSETb plasmid (Campbell *et al*., 2002), a gift from Dr. E. Cox (Princeton University). This cDNA was inserted into the NotI and XhoI sites of the STIM1 vector. A Kozac consensus sequence was inserted at the start codon to enhance expression, and inclusion of a stop codon on the 3′ tail of mRFP prevented expression of the myc and his epitope tags. Orai1/CRACM1 cDNA was encoded as a C-terminally FLAG-tagged construct in a pcDNA4 vector (Vig *et al*., 2006b). The fusion of Orai1 to the 3′ end of *Aequorea coerulescens* green fluorescent protein 1 (AcGFP) was constructed by cloning Orai1/CRACM1 from the pcDNA4 vector and inserting it into the BglII and KpnI sites of pAcGFP1-C1 (Clontech, Mountain View, CA). Mutants of Orai1/CRACM1 were constructed by overlap-extension polymerase chain reaction (PCR) and ligated into the BglII and KpnI sites of the pAcGFP1-C1 vector. A detailed description of the primers involved is included in Supplemental Materials. A plasmid containing cDNA for the phosphatidylinositol bisphosphate ($PIP_2$)-specific Pleckstrin homology (PH) domain from phospholipase C δ fused to the N terminus of enhanced (e)GFP (PH-eGFP; Várnai and Balla, 1998) was obtained from Dr. Andreas Jeromin (Allen Institute for Brain Science, Seattle WA). The construct ER-eGFP was constructed by ligation of the gene encoding the calreticulin ER localization sequence into the BglII and EcoRI sites and ligation of KDEL signal sequence into the BsrGI and NotI sites of pEGFP-N1 vector.

### *Cell Culture*

RBL-2H3 mast cells were cultured as monolayers in minimal essential medium supplemented with 1 μg/ml gentamicin and 20% (vol/vol) fetal bovine serum. In preparation for imaging, cells were harvested with trypsin/EDTA and passed at 25% confluence into 35-mm Mat-Tek dishes. After ~20 h, cells were transfected with fluorescent or epitope-tagged versions of STIM1 and Orai1/CRACM1. These constructs were cotransfected using either Geneporter (Genlantis, San Diego, CA) or FuGENE HD (Roche Diagnostics, Indianapolis, IN) per manufacturers' instructions, with modifications to enhance transfection efficiency in the RBL cells described previously (Gosse *et al*., 2005). Cells were sensitized with immunoglobulin E (IgE) by incubation with 650 ng/ml monoclonal anti-dinitrophenol (DNP) IgE overnight. Cells were imaged live or fixed 24 h after transfection.

COS7 cells were cultured as monolayers in DMEM supplemented with 1 μg/ml gentamicin and 10% (vol/vol) fetal bovine serum. In preparation for imaging, cells were harvested and transfected with FuGENE HD according to manufacturer's instructions.

### *Live Cell Imaging*

Immediately before imaging, RBL-2H3 cells were washed and incubated for 5 min at 37°C in 2.5 ml of buffered salt solution (BSS: 135 mM NaCl, 5 mM KCl, 1 mM $MgCl_2$, 5.6 mM glucose, 1 mg/ml bovine serum albumin [BSA], and 20 mM HEPES, pH 7.4) in the absence or presence of 1.8 mM $CaCl_2$, or $CaCl_2$ with or without 6 μM $GdCl_3$. Cells imaged in the presence of D-sphingosine, *N*,*N*-dimethylsphingosine (DMS), or *N*,*N*,*N*-trimethylsphingosine (TMS) (Avanti Polar Lipids, Alabaster, AL) were treated with 0.5 ml of BSS containing the compound (7.6 μM final concentration) immediately before imaging. Cells were then imaged on a TCS SP2 microscope with an APO 63× dipping objective (both from Leica Microsystems, Deerfield, IL). Cells were excited at 488 and 543 nm, with laser intensity and phototube sensitivity adjusted to maximize signal/noise. Fluorescence emission was monitored at 495–540 and 555–675 nm. All live cell imaging was carried out at 37°C. After observing the resting state of the cells, they were stimulated by the addition of 0.5 ml of BSS containing thapsigargin (150 nM final concentration) or multivalent antigen DNP-BSA (final concentration 3 nM in BSA). Leica Confocal software was used during the experiment to acquire images, and ImageJ (National Institutes of Heath Bethesda, MD) was used after acquisition to prepare composite micrographs by uniform contrast adjustment.

### *Calcium Measurements*

Immediately before imaging, COS7 cells were incubated with 0.9 μM fluo-4-acetoxymethyl ester (Invitrogen, Carlsbad, CA) for 10 min in BSS containing 0.5 mM sulfinpyrizone. Cell were then washed and resuspended in BSS/sulfinpyrazone. Fields of cells were imaged during thapsigargin stimulation with an Olympus APO 40× dipping objective, under the same conditions and settings as described for multicolor imaging. The increase in green fluorescence in the cell body due to stimulation with thapsigargin was quantified using ImageJ software. For calcium measurement in RBL-2H3 cells, indo-1 was loaded and monitored in a stirred cuvette by steady-state fluorometry as described previously (Pierini *et al*., 1997).

### *FRET Imaging*

RBL-2H3 cells were imaged for FRET by using the imaging system and cell preparation described above for multicolor live cell imaging. For cells stimulated with antigen, cytochalasin D (2 μM) was added immediately before imaging to minimize stimulated cell ruffling. Under these conditions, antigen stimulated $Ca^{2+}$ responses are slightly enhanced (Pierini *et al*., 1997). Cytochalasin D did not alter the FRET response to thapsigargin (data not shown). The Förster distance corresponding to the distance for 50% efficiency of FRET between eGFP and DsRed is calculated to be between 47 and 58 Å (Erickson *et al*., 2003), and this is expected to be similar for AcGFP and mRFP used in our measurements. Cross-sectional images of cells containing both protein constructs were monitored for fluorescence emission at 495–540 nm for AcGFP and 575–700 nm for mRFP (chosen to minimize bleed-through), by using an excitation wavelength of 476 nm. Irradiation at this wavelength provides adequate excitation of the AcGFP donor with negligible direct excitation of the mRFP acceptor. Laser intensity (set to minimize photobleaching of the donor), phototube sensitivity, and other settings remained constant for all FRET experiments. Throughout the time course of an individual experiment, images were taken simultaneously every 10 s for the red and green emission channels, and all FRET imaging was carried out at 37°C. Cells in 2.5 ml of BSS were treated with thapsigargin, DNP-BSA, $CaCl_2$, or $GdCl_3$ by addition of 0.5 ml of BSS containing each, similarly to live cell imaging experiments. Cells were treated with D-sphingosine, DMS, or TMS similarly by addition of 0.5 ml of BSS containing the sphingosine derivative immediately before the first image collected in each FRET sequence.

### *FRET Calculations*

The collected series of fluorescence images were quantified using a script written in MATLAB (Mathworks, Natick, MA) to determine the degree of FRET (see Supplemental Material). The script, based on previous analyses of FRET data (Guo *et al*., 1994, van Rheenen *et al*., 2004), begins by using the green channel image at each time point to make a mask of the pixels containing donor fluorescence (Das *et al*., 2008). Next, the integrated intensity of the pixels under the mask for each time point is calculated. Because the acceptor does not detectably colocalize with the donor before stimulation, the red pixel values before stimulation were attributed to bleed-through of donor fluorescence into the red channel. These prestimulation red and green integrated intensities were used to calculate the coefficient of bleed-through ($\beta$) by least squares analysis, accordingly to correct all other red channel integrated intensities for bleed-through. $\beta$ was found to be nearly constant at ~0.1 for all experiments. Last, the corrected ratio between the red and green integrated intensities at each time point was calculated as a relative measure of FRET according to the following equation (van Rheenen *et al*., 2004): $FRET = (M_A - \beta M_D)/M_D$, where $M_D$ is the measured donor fluorescence and $M_A$ is the measured acceptor fluorescence as integrated from the equatorial image at each time point. Both $M_D$ and $M_A$ are corrected by subtracting background pixel gray values. Time course data from individual cells (between 6 and 20 cells analyzed for each condition) were averaged, and these average time courses are plotted in Figures 4 and 5. The variation in protein expression for FRET measurements was quantified as a function of AcGFP fluorescence for the set of data used to calculate FRET after thapsigargin stimulation (Figure 4A). The expression levels of AcGFP-Orai1/CRACM1 and STIM1-mRFP are highly correlated between different cells (data not shown), so the measured AcGFP fluorescence provides an indication of expression levels for both proteins. As seen in Supplemental Figure S1, variation in the level of protein expression is >3-fold for these cells, but no correlation between expression levels and the magnitude of stimulated FRET was observed.

### *Online Supplemental Material*

Supplemental Methods available online include the primer sequences used in cloning, description of the results shown in Supplemental Figure S5, Supplemental Figures S1–S5, and the annotated MATLAB script used to quantify image data for FRET measurement.

## RESULTS

### *STIM1 Redistribution upon Thapsigargin Stimulation Is Accompanied by Rearrangement of the ER in RBL Mast Cells*

Previous reports indicated that the subcellular localization of STIM1 in unstimulated cells depends on microtubules (Baba *et al*., 2006; Mercer *et al*., 2006) and that STIM1 colocalizes with an ER marker (Liou *et al*., 2005; Wu *et al*., 2006). In unstimulated RBL cells, STIM1-mRFP substantially colocalizes with $\alpha$-tubulin-eGFP (Supplemental Figure S2). To evaluate spatial relationships to ER components in RBL cells, STIM1-mRFP and ER-eGFP, a luminally targeted protein, were transiently coexpressed. In unstimulated cells, STIM1-mRFP shows very limited colocalization with ER-eGFP, largely because of its greater microtubule association than this luminal ER marker (Figure 1A). However, upon stimulation with thapsigargin, STIM1-mRFP and ER-eGFP become more extensively colocalized in reticulated, micrometer-sized sheets of ER membrane (Figure 1B). Under these conditions, microtubule association of STIM1 seems reduced (data not shown). Similar results are obtained when the subcellular distributions STIM1-mRFP are compared with the endogenous luminal ER marker, protein disulfide isomerase, before and after thapsigargin treatment (data not shown). These results are consistent with ER localization of STIM1 and preferential association with microtubules before stimulation. They also show the capacity of thapsigargin to induce large-scale ER rearrangement.

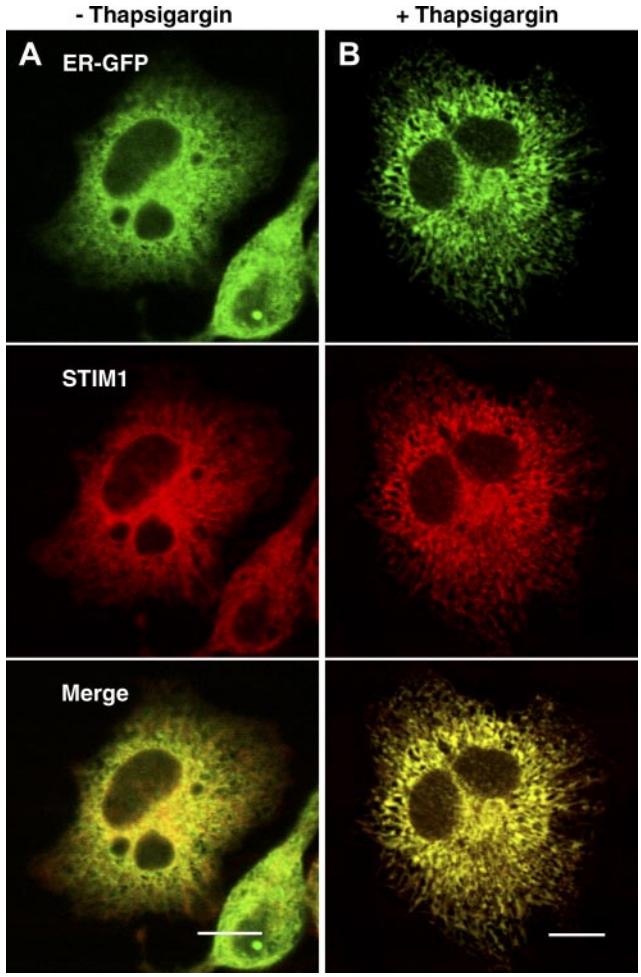


**Figure 1.** RBL mast cell expressing STIM1-mRFP (red) and ER-eGFP (green) exhibits stimulation-dependent changes in localization of these proteins. Representative cells are shown before (A) and after (B) stimulation with thapsigargin. Note the extension of the ER network throughout the cytoplasm after stimulation and the increased colocalization of STIM1 with the luminal ER marker. Bars, 10 $\mu$m.

### *STIM1 and Orai1/CRACM1 Coredistribute to Micrometer-sized Dorsal Membrane Patches Due to Stimulation by Thapsigargin*

Previous reports documented the localization of Orai1/CRACM1 at the plasma membrane (Vig *et al*., 2006b) and its coredistribution with STIM1 into plasma membrane-associated punctae in response to thapsigargin (Liou *et al*., 2005; Luik *et al*., 2006). We find in RBL cells that STIM1-mRFP and AcGFP-Orai1/CRACM1 coredistribute into a mosaic pattern at the dorsal cell surface as early as 1 min after addition of thapsigargin, and this pattern remains stable for more than several minutes (Figure 2). The time course we observe correlates with the time dependence of SOCE after thapsigargin-stimulated release from stores in these cells (Glitsch and Parekh, 2000). These micrometer-sized patches at the dorsal cell surface are larger than punctae initially reported for ventral surface confocal (Liou *et al*., 2005) or total internal reflection fluorescence (TIRF) images (Wu *et al*., 2006), but these dorsal-localized patches are similar in size as other STIM1-Orai1/CRACM1 patches observed by confocal microscopy in several recent studies in other cell types (Varnai *et al*., 2007; Smyth *et al*., 2008). Moreover, using TIRF microscopy at the ventral cell surface of RBL cells, we observe the formation of smaller submicron-scale STIM1-mRFP AcGFP-Orai1/CRACM1 punctae in response to thapsigargin, and these are similar to those observed in other studies (Liou *et al*., 2005; Wu *et al*.,2006) (Supplemental Figure S3). Our results establish that, in response to thapsigargin, STIM1-mRFP and AcGFP-Orai1/CRACM1 expressed transiently in RBL cells undergo large-scale coredistribution that is qualitatively similar to that observed for other fluorescent derivatives of these proteins in other cell types.

### *Antigen-stimulated Coredistribution of Orai1/CRACM1 and Stim1is Highly Restricted Compared with That Stimulated by Thapsigargin*

We found only limited coredistribution of STIM1-mRFP and AcGFP-Orai1/CRACM1 after stimulation mediated by IgE-receptors after cross-linking by multivalent antigen. Under these conditions, AcGFP-Orai1/CRACM1 remains at the plasma membrane and is evident in the stimulated membrane ruffles (Figure 3A). Furthermore, STIM1-mRFP shows only dim localization with AcGFP-Orai1/CRACM1 in these ruffles, and the degree of translocation to the plasma membrane is substantially less than that seen with thapsigargin stimulation (Figure 2; also see below). This was not expected, in part because of the well-documented activation of $I_{CRAC}$ activation by antigen in RBL cells (Hoth and Penner, 1992; Zhang and McCloskey, 1995; McCloskey and Zhang, 2000). Furthermore, the $Ca^{2+}$ response to antigen is 71 $\pm$ 14% of that caused by thapsigargin during 5 min of activation (Supplemental Figure S4A and B; data not shown).

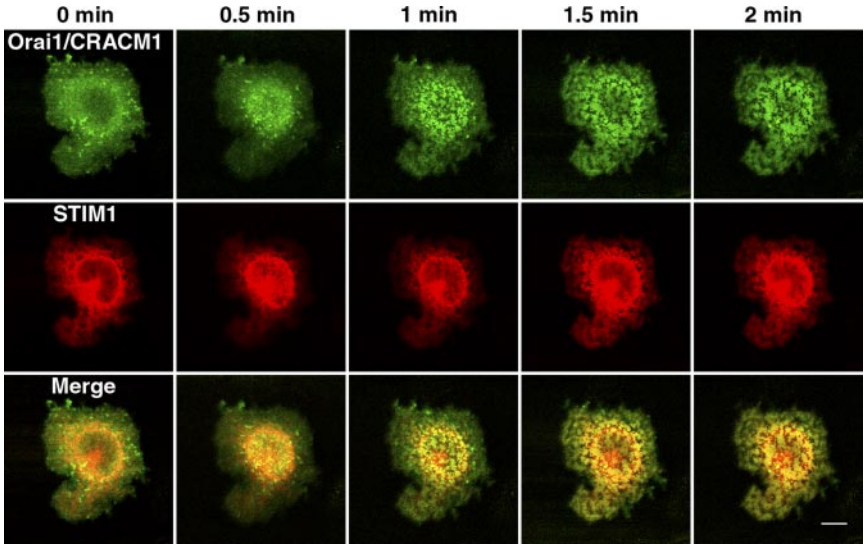


**Figure 2.** Time course of AcGFP-Orai1/CRACM1 (green) and STIM1-mRFP (red) formation of colabeled plasma membrane domains after thapsigargin stimulation. The patches seen in the last image, formed after 2 min of stimulation, remained relatively unchanged for an additional 10 min (not shown). Dorsal cell surface images. Bar, 10 $\mu$m.

This striking difference between stimulation of STIM1-Orai1/CRACM1 coredistribution by thapsigargin and antigen points to differences in mechanism, and in particular, that thapsigargin operates by inhibiting SERCA, thereby preventing refilling of ER $Ca^{2+}$ stores. In contrast, antigen stimulation does not impose this restriction. We could evaluate the significance of $Ca^{2+}$ influx during antigen stimulation by using two different conditions to prevent it: elimination of $Ca^{2+}$ in the extracellular buffer and addition of $GdCl_3$ to block $I_{CRAC}$ (Dellis *et al*., 2006). We found that RBL cells stimulated by antigen under either of these conditions show redistributions of STIM1 and CRACM1 similar to cells stimulated with thapsigargin. In the absence of extracellular $Ca^{2+}$ (Figure 3B) or in the presence of 6 $\mu$M $GdCl_3$ (Figure 3C), antigen stimulation causes STIM1-mRFP to localize to domains that also contain AcGFP-Orai1/CRACM1. We confirmed that under these conditions, $Ca^{2+}$ mobilization is substantially reduced (Supplemental Figure S4C and D).

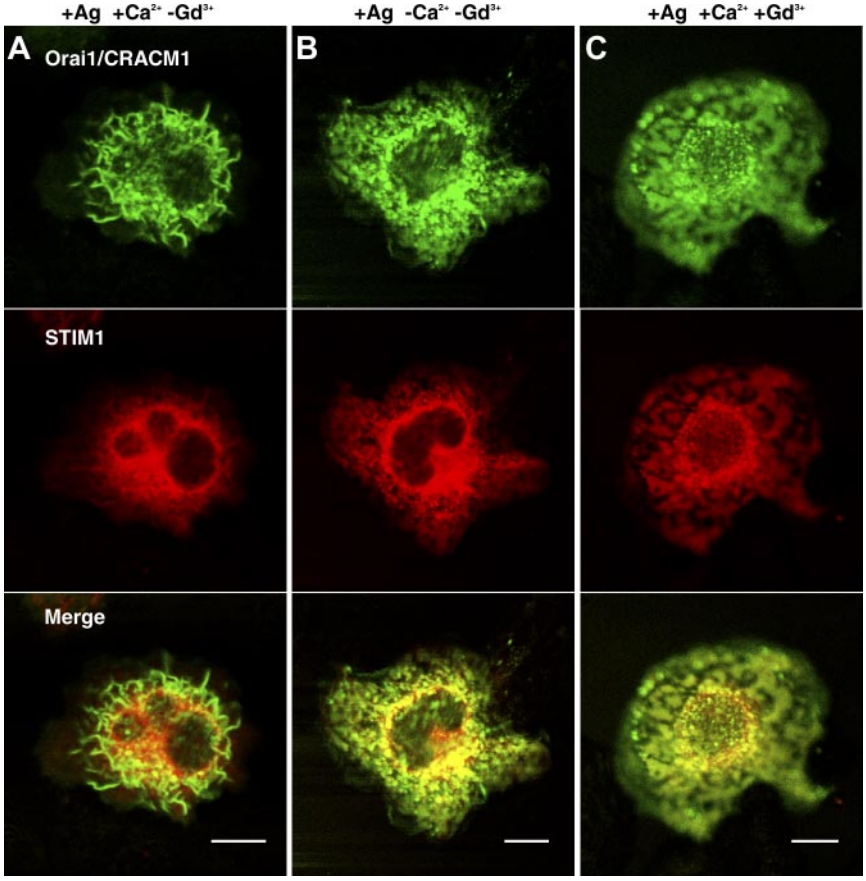


**Figure 3.** Confocal images of AcGFP-Orai1/CRACM1 (green) and STIM1-mRFP (red) in dorsal slices of RBL mast cells stimulated with antigen under different conditions affecting calcium influx. Cell stimulated in BSS buffer with (A) and without (B) $CaCl_2$. (C) Cell stimulated in BSS with $Ca^{2+}$ and 6 $\mu$M $GdCl_3$. Bars, 10 $\mu$m.

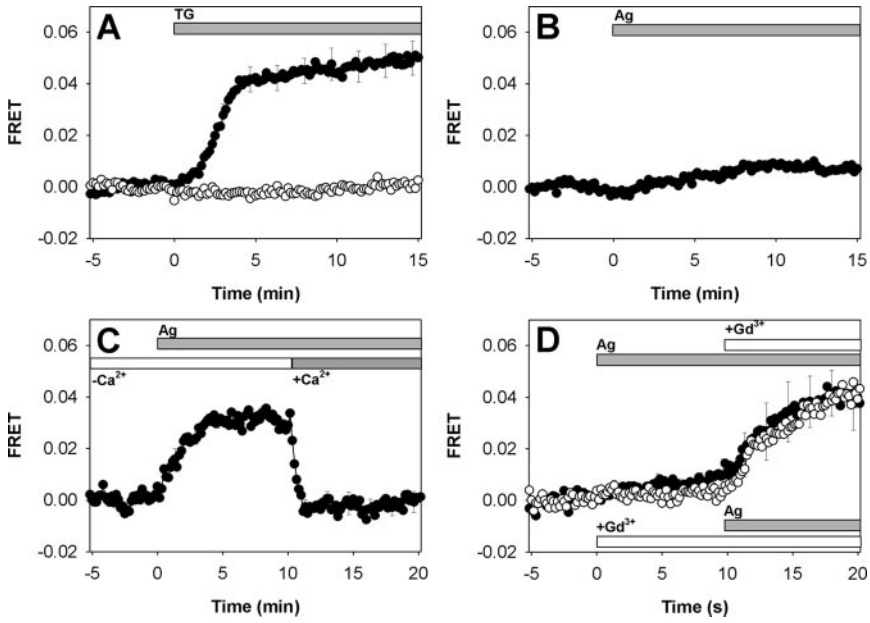


**Figure 4.** FRET between AcGFP-Orai1/CRACM1 and STIM1-mRFP in plasma membrane of RBL mast cells. (A) FRET after addition of 150 nM thapsigargin (indicated by bar) to labeled cells (solid circles; error bars show SEM) compared with control cells expressing PH-eGFP and unlabeled Orai1/CRACM1 instead of AcGFP-Orai1/CRACM1 (open circles, SEM $\sim 2.0 \times 10^{-3}$). (B) FRET after antigen stimulation with 3 nM DNP-BSA in BSS (SEM $\sim 1.0 \times 10^{-3}$). (C) FRET after same antigen stimulation but in the absence of extracellular $Ca^{2+}$. $CaCl_2$ (1.8 mM) was restored as indicated by bar (error bars show SEM). (D) FRET after stimulation by antigen followed by addition of 6 $\mu$M $GdCl_3$ (solid circles; top bars; error bars show SEM; solid line) or after $GdCl_3$ addition followed by antigen stimulation (open circles; bottom bars; error bars omitted; dotted line).

Thus, our imaging results indicate that persistent store depletion is necessary for stable, large-scale coredistribution of STIM1 and Orai1/CRACM1. This occurs with SERCA2 inhibition by thapsigargin but not with stimulation by antigen in the presence of extracellular $Ca^{2+}$, which causes more dynamic and/or less complete store depletion.

Equatorial confocal images clearly distinguish the distribution of these labeled proteins at the plasma membrane verses the cytoplasm, and similar conclusions are reached (Supplemental Material and Supplemental Figure S5A). Furthermore, comparison of the distribution of AcGFP-Orai1/CRACM1 to the plasma membrane marker Alexa555-cholera toxin B in equatorial images shows that Orai1/CRACM1 associated with STIM1 is localized to the nonruffled regions of the plasma membrane (Supplemental Figure S5B). Overall, our microscopy results support previous conclusions that $Ca^{2+}$ depletion from stores causes STIM1 and Orai1/CRACM1 to coredistribute in large domains at the plasma membrane, and they also elucidate the reversal or restriction of this process that is related to store refilling by $Ca^{2+}$ influx.

### *FRET Measurements Reveal Close Interactions between STIM1-mRFP and AcGFP-Orai1/CRACM1 That Are Sustained If Stores Are Not Refilled*

Visualized colocalization of STIM1 with Orai1/CRACM1 at the plasma membrane (Figures 2 and 3 and Supplemental Figure S5A) is limited by optical resolution (>200 nm). To assess whether these proteins become close enough for direct interaction, we monitored changes in FRET from the donor AcGFP-Orai1/CRACM1 to the acceptor STIM1-mRFP in response to stimulation. The distance sensitivity of these measurements is represented by the Förster distance, which for this donor-acceptor pair is estimated to be ~5 nm (Erickson *et al*., 2003). Equatorial images were evaluated, with an image mask to isolate the fluorescence associated with the plasma membrane for each cell and time point. The ratio of corrected red (acceptor) fluorescence to the green (donor) fluorescence provides a relative measure of FRET as described in the equation under *Materials and Methods*.

Thapsigargin added to cells expressing STIM1-mRFP and AcGFP-Orai1/CRACM1 causes a robust increase in FRET on the time scale of several minutes. Figure 4A shows this time course derived from image analyses of individual cells and averaged over 18 representative cells. After a lag period of up to 100 s, FRET increases to a relatively constant value with an average half time of ~180 s. This lag most likely reflects the period during which $Ca^{2+}$ in ER stores is reduced, and the time dependent increase in FRET intensity is consistent with the time course for activation of $Ca^{2+}$ influx that may be limited by the rate of STIM1 redistribution. These FRET results are consistent with fluorescence micrographs showing STIM1 and Orai1/CRACM1 colocalization in response to thapsigargin stimulation (e.g., Figure 2 and Supplemental S5A), and they reveal further that these SOCE components from ER and plasma membrane, respectively, are interacting stably in proximity (≤10 nm) under conditions where store refilling is prevented.

An important control to distinguish measured FRET from increases in acceptor fluorescence due to recruitment of STIM1-mRFP to the plasma membrane is to substitute AcGFP-Orai1/CRACM1 with another plasma membrane-localized GFP-labeled protein that does not associate directly with STIM1-mRFP. For this purpose, we used eGFP linked to the $PIP_2$-binding PH domain of phospholipase C δ (PH-eGFP). PH-eGFP strongly localizes to the plasma membrane in these cells in the presence and absence of thapsigargin, similar to AcGFP-Orai1/CRACM1 (Wu *et al*., 2004; data not shown). STIM1-mRFP, cotransfected with PH-eGFP and nonfluorescent Orai1/CRACM1, exhibits thapsigargin-stimulated translocation to patches at or near the plasma membrane, and this fluorescence is visualized by microscopy to be colocalized with uniformly-distributed PH-eGFP (data not shown). However, no change in FRET is detected between PH-eGFP and STIM1-mRFP in response to thapsigargin (Figure 4A).

In contrast to thapsigargin-stimulated FRET, only a small, time-dependent increase in FRET between AcGFP-Orai1/CRACM1 and STIM1-mRFP is caused by antigen (Figure 4B), consistent with the very limited redistribution of STIM1-mRFP to the plasma membrane visualized microscopically in response to antigen (Figure 3A and Supplemental Figure S5A). Because robust SOCE is observed in

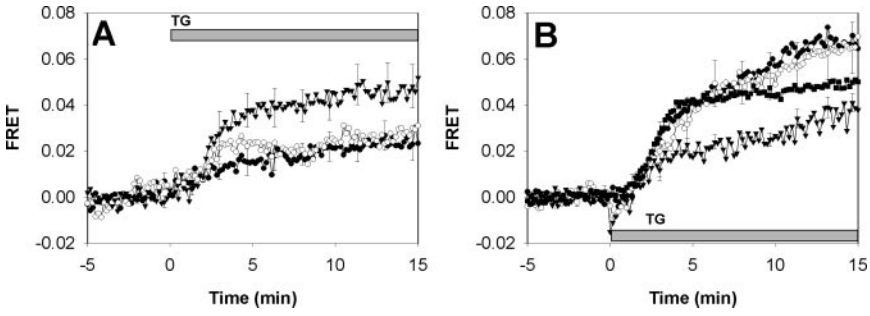


**Figure 5.** (A) Thapsigargin-stimulated FRET between AcGFP-Orai1/CRACM1 and STIM1-mRFP in the presence of D-sphingosine (7.6 μM, open circles), DMS (7.6 μM, closed circles; error bars omitted), and TMS (7.6 μM, triangles). (B) Thapsigargin-stimulated FRET between STIM1-mRFP and AcGFP-Orai1/CRACM1 (squares, same as Figure 4A, shown for comparison; error bars omitted), AcGFP-Orai1/CRACM1ΔD (closed circles; error bars omitted), AcGFP-Orai1/CRACM1ΔE (open circles), and AcGFP-Orai1/CRACM1ΔDE (triangles). Error bars show SEM.

RBL cells after antigen stimulation (Supplemental Figure S4), the results indicate that efficient SOCE can be achieved with more limited STIM1-Orai1/CRACM1 interactions than those observed with thapsigargin. We hypothesize that dynamic emptying and refilling of stores that occurs as part of this mechanism is manifest as more transient and/or local store depletion and consequently more limited STIM1 redistribution to the plasma membrane.

To test this hypothesis, we stimulated cells with antigen in the absence of extracellular $Ca^{2+}$ to prevent refilling of stores. We observed a time-dependent increase to a large, sustained level of FRET between Orai1/CRACM1-AcGFP and STIM1-mRFP that is rapidly reversed ($t½ < 30s$) when millimolar $Ca^{2+}$ is added back (Figure 4C). This FRET measurement is again consistent with visualization by microscopy (Figure 3B and Supplemental S5A), and it further demonstrates nanoscale proximity of STIM1 and Orai1/CRACM1 due to receptor-mediated cell activation. Under these conditions, we observe redistribution of STIM1 away from the plasma membrane that is slower than the reversal of FRET, taking 1–3 min to complete (data not shown). This difference suggests that the rate of redistribution of STIM1-mRFP uncoupled from its interaction with Orai1/CRACM1 is limited by its diffusion in the ER membranes, consistent with recent observations of Liou *et al*. (2007).

To investigate whether the close interaction between Orai1/CRACM1 and STIM1 is sensitive to $Ca^{2+}$ influx mediated by $I_{CRAC}$ specifically, we examined the effect of $GdCl_3$ on the measured FRET. After 10 min of antigen stimulation that caused only a small increase in FRET, addition of 6 μM $GdCl_3$ resulted in a time-dependent increase in FRET that approached a steady-state value after 10 min and was similar in magnitude to that for antigen stimulation in the absence of $Ca^{2+}$ (Figure 4D, closed circles). Similar results were obtained when cells were pretreated with $GdCl_3$ and subsequently stimulated with antigen (Figure 4D, open circles). Evidently, $GdCl_3$-mediated inhibition of SOCE is sufficient to sustain Orai1/CRACM1-STIM1 interactions similarly to thapsigargin. These FRET results provide a nanoscale view of the interactions between Orai1/CRACM1 and STIM1 in antigen-stimulated cells that are dynamically regulated by ER luminal $Ca^{2+}$ levels.

### *D-Sphingosine and N,N*-Dimethylsphingosine Inhibit the Association between STIM1 and Orai1

A previous study demonstrated the capacity of D-sphingosine and its derivative DMS to inhibit inositol trisphosphate ($IP_3$)-elicited $I_{CRAC}$ in RBL mast cells (Mathes *et al*., 1998). To investigate whether sphingosine or DMS directly affects the interaction between STIM1 and Orai1/CRACM1 we measured FRET between AcGFP-Orai1 and STIM1-mRFP in the presence of 8 μM D-sphingosine or DMS after thapsigargin stimulation. These conditions are sufficient for inhibition of >60% of thapsigargin-stimulated $Ca^{2+}$ influx by these amphiphiles (Figure 6A). As shown in Figure 5A, we find that both D-sphingosine and DMS strongly inhibit the interaction between STIM1 and Orai1/CRACM1. In contrast, *N,N,N*-trimethylsphingosine, the quarternary amine derivative of D-sphingosine, does not significantly reduce the FRET response to thapsigargin compared with untreated cells (Figure 4) and does not inhibit SOCE (Figure 6A). In other studies, we find that all three of these amphiphiles efficiently insert into the outer leaflet of the plasma membrane, but only D-sphingosine and DMS can flip to the inner leaflet (Smith, Baird, and Holowka, unpublished data), where they can directly interfere with the STIM1-Orai1/CRACM1 interaction. These results suggest the possibility of direct, electrostatic interference by D-sphingosine and DMS of the interaction between STIM1 and Orai1/CRACM1. The capacity of these positively charged lipids with different headgroup structures to similarly inhibit this interaction is more consistent with an electrostatic mechanism than a specific binding interaction. Moreover, addition of both D-sphingosine and DMS induce the formation of large

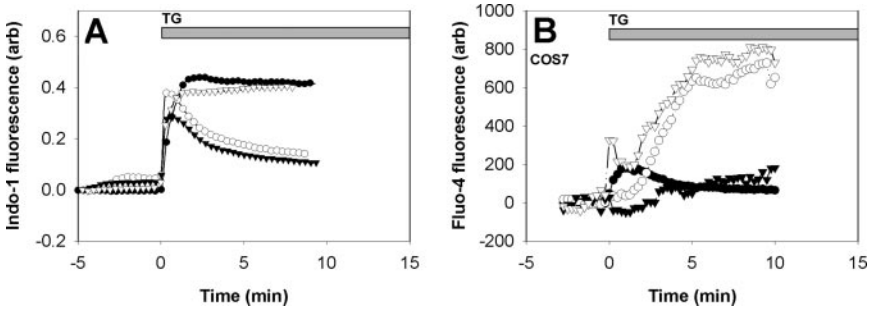


**Figure 6.** (A) Effects of sphingosine derivatives on thapsigargin induced $Ca^{2+}$ mobilization, indo-1-monitored. $Ca^{2+}$ response of suspended RBL cells for untreated cells (closed circles), cells in the presence of D-sphingosine (7.6 μM, open circles), DMS (7.6 μM, closed triangles), TMS (7.6 μM, open triangles). Every 10th data point is shown for clarity. (B) Calcium measurements of COS7 cells monitored by fluo-4 imaging. Thapsigargin mediated $Ca^{2+}$ mobilization is shown for untransfected cells (closed circles), cells expressing STIM1-mRFP with AcGFP-Orai1/CRACM1 (open circles), AcGFP-Orai1/CRACM1ΔE (open triangles), and AcGFP-Orai1/CRACM1ΔDE (closed triangles).

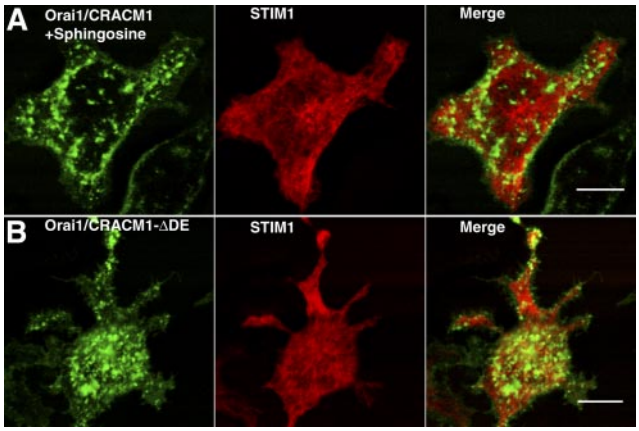


**Figure 7.** (A) AcGFP-Orai1/CRACM1 in the presence of 7.6 $\mu$M D-sphingosine exhibits plasma membrane patches without STIM1-mRFP redistribution. (B) AcGFP-Orai1/CRACM1ΔDE and STIM1-mRFP exhibits plasma membrane patches without STIM1-mRFP redistribution. Compare these dorsal surface images to Figure 3, t = 0. Bars, 10 $\mu$m.

patches of Orai1/CRACM1 without colocalization of STIM1 (Figure 7A). Other plasma membrane proteins, such as FcεRI, do not detectably cluster under these conditions (data not shown). These results show that not only do these sphingosine derivatives disrupt the stimulated interaction between STIM1 and Orai1/CRACM1, but they also induce selective aggregation of Orai1/CRACM1.

### *Charged Amino Acid Residues in the C Terminus of Orai1/CRACM1 Are Important for Its Interaction with STIM1*

A recent study provided evidence for the role of a coiled-coil domain at the C terminus of Orai1/CRACM1 in the interaction between this protein and STIM1 (Muik *et al.*, 2008). This domain contains a series of three aspartates (D284, D287, and D291) and a separate series of three glutamates (E272, E275, and E278) predicted to be on the hydrophilic face of the coiled-coil. We probed the importance of charge on these six amino acids by constructing three separate AcGFP-Orai1/CRACM1 mutants in which all three aspartates are converted to asparagine (AcGFP-Orai1/CRACM1ΔD), all three glutamates are converted to glutamine (AcGFP-Orai1/CRACM1ΔE), or all six acidic amino acids are changed to their neutral analogues (AcGFP-Orai1/CRACM1ΔDE). We then monitored FRET between STIM1-mRFP and the AcGFP-Orai1/CRACM1 mutants and compared this to the FRET between STIM-mRFP and wild-type AcGFP-Orai1/CRACM1 described above. As shown in Figure 5B, neutralization of three of the six acid residues resulted in an increase in thapsigargin-stimulated FRET at longer times, whereas the neutralization of all six acidic residues resulted in a significant decrease in stimulated FRET. Moreover, cells expressing AcGFP-Orai1/CRACM1ΔDE exhibited large patches of this protein in the absence of stimulated clustering of STIM1, similar to cells treated with D-sphingosine or DMS (Figure 7B). These results suggest that D-sphingosine and DMS promote Orai1/CRACM1 clustering by neutralization of the negative charges in the putative coiled-coil at the C terminus of this protein, and in so doing they prevent its interaction with the C terminus of STIM1 under cell-activating conditions, possibly via its positively charged polybasic sequence (Li *et al.*, 2007).

### *Charged Amino Acid Residues in the C Terminus of Orai1/CRACM1 Are Important for Functional CRAC Influx*

Because RBL cells have a large endogenous SOCE response, the functional consequences of mutations were examined in COS7 cells. The $Ca^{2+}$ response to thapsigargin was monitored in COS7 cells transiently expressing STIM1-mRFP and AcGFP-Orai1/CRACM1 or one of the Orai1/CRACM1 mutants. COS7 cells exhibit relatively limited SOCE that is substantially enhanced by expression of STIM1-mRFP and AcGFP-Orai1/CRACM1 (Figure 6B, open circles). Potentiation of SOCE due to overexpression of STIM1 and Orai1/CRACM1 has been reported previously in COS7 cells (Varnai *et al.*, 2007), and our results demonstrate the functional competence of STIM1-mRFP and AcGFP-Orai1/CRACM1 used in our FRET measurements. Cells expressing AcGFP-Orai1/CRACM1ΔE show a potentiation of $Ca^{2+}$ influx similar to that observed with wild-type Orai1/CRACM1. In contrast, cells expressing AcGFP-Orai1/CRACM1ΔDE and STIM1-mRFP show only a very slow, small increase in $Ca^{2+}$ in response to thapsigargin (Figure 6B). Moreover, these cells show a substantially delayed or reduced calcium release from stores compared with untransfected COS7 cells. This observation indicates that these acidic residues on Orai1/CRACM1 can influence the sensitivity of these cells to thapsigargin mediated $Ca^{2+}$ release from stores. These $Ca^{2+}$ mobilization results correlate with the reduction in FRET observed with AcGFP-Orai1/CRACM1ΔDE (Figure 5B), indicating that the negatively charged residues in the C terminus of Orai1/CRACM1 are important for functional SOCE.

## DISCUSSION

Our FRET measurements in conjunction with fluorescence confocal imaging reveal molecular interactions between Orai1/CRACM1 and STIM1 that are regulated by dynamic depletion and refilling of intracellular $Ca^{2+}$ stores. Whereas thapsigargin inhibition of store refilling results in extensive association of Orai1/CRACM1 and STIM1, the SERCA-mediated store refilling that occurs normally during antigen stimulation substantially limits these molecular interactions. Additionally, our results show that store depletion results in the remodeling of the ER that accompanies redistribution of STIM1. STIM1 was previously identified as a transmembrane protein that colocalizes with the ER in unstimulated cells (Liou *et al.*, 2005; Wu *et al.*, 2006), whereas more recent studies have found STIM1 colocalization with microtubules (Baba *et al.*, 2006; Mercer *et al.*, 2006). Our results with RBL mast cells provide visual evidence that localization of STIM1 in unstimulated cells is templated to a large extent by microtubules, and this differs from luminal ER-localized fluorescent proteins, which show little or no microtubule association (Figure 1A and Supplemental S2).

It is not yet clear whether STIM1 associated with microtubules is preferentially recruited to the plasma membrane in stimulated cells, but we observe a reduction in microtubule-associated STIM1-mRFP upon thapsigarin treatment (Figure 1; data not shown). Baba *et al.*, (2006) showed that GFP-STIM1–containing tubulovesicular structures rapidly move along microtubule tracks in DT40 B cells, and treatment of nocodazole to depolymerize microtubules halted this rapid movement but did not inhibit B cell receptor-stimulated SOCE. In another study, Smyth *et al.*, (2007) showed that enhanced yellow fluorescent protein (eYFP)-STIM1 associates with microtubules in HEK293 cells and that nocodazol inhibition substantially inhibits thapsigargin-

stimulated CRAC influx in these cells in the absence of eYFP-STIM1 expression.

Our observation that intracellular localization of STIM1 changes dramatically upon stimulation of RBL cells with thapsigargin is consistent with results reported for other cell types (Liou *et al*., 2005; Wu *et al*., 2006). We find that the distribution of both STIM1-mRFP and ER-eGFP seem to change, such that cytoplasmically localized STIM1-mRFP and ER-eGFP become more extensively colocalized in the variegated network of the ER (Figure 1B). The rearrangement of the ER network upon thapsigargin stimulation is consistent with the previously reported role of STIM1 in the microtubule assisted remodeling of the ER (Grigoriev *et al*., 2008). In addition to this cytoplasmically localized STIM1-mRFP, a pool of STIM1-mRFP redistributes to the plasma membrane to form an extended network that colocalizes with AcGFP-Orai1/CRACM1 (Figure 2). Equatorial sections show that this network of plasma membrane-associated STIM1-mRFP localizes to the flat regions of the plasma membrane between ruffles and other protrusions that are labeled by the plasma membrane marker $A^{555}$-CTB (Supplemental Figure S5B). This mosaic of plasma membrane-STIM1/ER junctions at the dorsal cell surface clearly represents a large percentage of the plasma membrane surface area under conditions of stimulation by thapsigargin in these cells. These results do not seem to be a consequence of overexpression of these proteins, as they are observed over a wide range of expression levels. Furthermore, expression of these proteins does not significantly alter $Ca^{2+}$ responses to antigen or thapsigargin in these cells (data not shown). The size of the dorsal domains observed is consistent with Orai1/CRACM1-STIM1 patches reported in some other studies (Varnai *et al*., 2007; Smyth *et al*., 2008). More discrete punctae of STIM1 are observed at the ventral cell surface by TIRF microscopy (Supplemental Figure S3) similar to those seen in other reports in these (Liou *et al*., 2007) and other cells by both confocal (Liou *et al*., 2005, 2007) and TIRF microscopy (Wu *et al*., 2006; Liou *et al*., 2007).

To examine the molecular interactions of STIM1 and Orai1/CRACM1, we developed a microscopy-based FRET assay that is computationally similar to the membrane colocalization assay recently established in our laboratory (Das *et al*., 2008). Our experimental system and membrane localized FRET analysis allowed the measurement of the interaction between STIM1-mRFP and AcGFP-Orai1/CRACM1 with high sensitivity, temporal resolution, and reproducibility. A distinct advantage of the AcGFP/mRFP donor/acceptor pair is that excitation of the green donor with the 476 nm laser line initiates energy transfer with negligible direct excitation of the red acceptor fluorophore, thus simplifying the FRET computation, which is targeted by automated masking of equatorial plasma membrane as the selected region of interest. Because selection of the measured regions of interest is automated on a frame-by-frame basis, the ratiometric analysis of energy transfer (see equation under *Materials and Methods*) is insensitive to variations in the focal plane and laser intensity, as well as morphological differences between cells. Individual cells are imaged over time (before and after stimulation), and the FRET time courses for multiple cells are averaged.

Previous TIRF imaging of thapsigargin-stimulated cells showed optical colocalization of labeled STIM1 and Orai1/CRACM1 in plasma membrane punctae (Luik *et al*., 2006), and further evidence for molecular level interactions comes from coimmunoprecipitation of STIM1 with Orai1/CRACM1 in complexes derived from lysates of thapsigargin-stimulated cells (Yeromin *et al*., 2006). Our FRET measurements demonstrate that labeled STIM1 and Orai1/CRACM1 interact closely at the plasma membrane of live cells as a consequence of store depletion, and they are consistent with these two proteins associating directly to facilitate the CRAC response. These measurements detect proximity on the order of 5 nm but do not rule out the participation of other molecular components in this interaction. A recent study in HEK293 cells provided FRET evidence interactions between STIM1-eYFP and eCFP-Orai1/CRACM1 after store depletion by SERCA inhibitors (Muik *et al*., 2008). Barr *et al*. (2008) detected FRET between these proteins stimulated by surface-associated T cell receptor ligands, but they did not compare the magnitude of this FRET to that induced by SERCA inhibition. In contrast, Varnai *et al*. (2007) showed that interactions between STIM1 and Orai1/CRACM1 detected by confocal microscopy were excluded from plasma membrane regions that were bridged to ER-tethering proteins estimated to provide $<6$ nm of intermembrane spacing. They suggested that interactions between STIM1 and Orai1 involve additional proteins that extend spacing between the PM and ER to $>8$ nm, but alternative explanations for these observations, such as orientational or electrostatic interference by the bridging proteins, cannot be excluded.

Unexpectedly, antigen stimulation of RBL cells leads to STIM1 and Orai1/CRACM1 interactions at the plasma membrane that are highly restricted, as observed with both confocal imaging (Figure 3A) and FRET (Figure 4B). The striking difference from thapsigargin stimulation can be explained by dynamic refilling of intracellular $Ca^{2+}$ stores by influx that accompanies antigen stimulation and is prevented when the SERCA pumps are blocked by thapsigargin. Thus, dynamic refilling of $Ca^{2+}$ stores apparently resets the baseline and reverses the interaction between STIM1 and Orai1/CRACM1. Consistent with this hypothesis, stimulation with antigen under conditions that prevent refilling of stores, either the absence of extracellular $Ca^{2+}$ or the presence of $Gd^{3+}$ to block CRAC-mediated $Ca^{2+}$ entry, results in strongly enhanced interactions very similar to those observed with thapsigargin. Specifically, extensive colocalization of labeled STIM1 and Orai1/CRACM1 occurs at the plasma membrane as visualized with confocal microscopy (Figure 3, B and C, and Supplemental Figure S5A) and substantially increased molecular interactions are detected with FRET (Figure 4, C and D). Other recent reports are consistent with these observations. Muik *et al*. (2008) showed that FRET between STIM1-CFP and Orai1-YFP stimulated by agonist together with a weak SERCA inhibitor in the absence of $Ca^{2+}$ was reversed by $Ca^{2+}$ addition in HEK293 cells; Varnai *et al*. (2007) showed that ATP-stimulated STIM1 recruitment to the plasma membrane in COS7 cells was reversed by extracellular $Ca^{2+}$; and Smyth *et al*. (2008) showed that carbacol-induced STIM1/Orai1 punctae formation detected by TIRF in HEK293 cells was reversed by $Ca^{2+}$ addition. Our results highlight the physiological regulation of this interaction when stimulated by an immunoreceptor, FcεRI, during mast cell activation.

It is notable that the kinetics of the molecular association between STIM1 and Orai1/CRACM1, which increases to a steady-state with a half-time of several minutes, are similar whether $Gd^{3+}$ is added before or after antigen to initiate the response (Figure 4D). Thus, it seems that the rate-limiting step in this process is the redistribution of STIM1 to the plasma membrane, rather than preceding steps of antigen-stimulated signaling. In contrast, addition of extracellular $Ca^{2+}$ to antigen-stimulated cells causes a rapid reduction in FRET, occurring with a half time of $\sim$20 s (Figure 5C),

suggesting that stores are refilled very rapidly under these conditions. These results support the view that molecular interactions between STIM1 and Orai1/CRACM1 that are stimulated by antigen are highly dynamic and readily reversed by store refilling. Our FRET results provide a somewhat different picture than those of Liou *et al*. (2007), who monitored FRET between CFP-STIM1 and YFP-STIM1 in RBL mast cells and observed increases that were similar for antigen and thapsigargin stimulation. They monitored STIM1/STIM1 interactions throughout the ER, and their data show that these interactions are initiated before localization of STIM1 in plasma membrane punctae. These STIM1-STIM1 interactions possibly depend differently on store depletion/refilling than do STIM1-Orai1/CRACM1 interactions. Direct measurement of intraluminal free $Ca^{2+}$ in the ER under different conditions of stimulation may help to address this question.

Inhibition of thapsigargin-stimulated FRET between Ac-GFP-Orai1/CRACM1 and STIM1-mRFP by D-sphingosine and DMS is consistent with the inhibitory effects of these amphiphiles on $IP_3$-mediated store-operated $Ca^{2+}$ (SOC) influx in RBL cells (Mathes *et al*., 1998). We confirmed that these molecules show a similar inhibitory effect on thapsigargin mediated SOCE in these cells (Figure 6). TMS does not significantly inhibit the interaction between Ac-GFP-Orai1/CRACM1 and STIM1-mRFP, and it seems likely that D-sphingosine and DMS are effective because of the net increase in positively charged lipids that they provide upon flipping to the inner leaflet of the plasma membrane (Smith, unpublished data; Sato *et al*., 2006). Although DMS is a well-known inhibitor of sphingosine kinases (Yatomi *et al*., 1996), it is unlikely that its effect on FRET depends on inhibition of this enzyme family, because the substrate for these enzymes, D-sphingosine, is equally effective in inhibiting FRET (Figure 5A) and $Ca^{2+}$ influx (Figure 6A). We hypothesize that D-sphingosine and DMS at the inner leaflet electrostatically interact with six acidic residues at the C terminus of Orai1/CRACM1 to prevent the interaction of these residues with STIM1 under conditions of CRAC activation. This model is in contrast to those published in recent reports by Peinelt and Smyth in which pharmacological agents disrupt the interaction of STIM1 with Orai1/CRACM1 by reversing the store-dependent multimerization and translocation of STIM1 (Peinelt *et al*., 2008; Smyth *et al*., 2008). It is possible that the effects of these positively charged amphiphiles directly prevent the association with STIM1, or that this effect is mediated by alteration of the lipid environment, thereby preventing the association of Orai1/CRACM1 with STIM1. In this regard, electrostatic neutralization of negatively charged phospholipids, such as phosphoinositides, by these positively charged amphiphiles could play a role in their mechanism of inhibition. The hypothesis that this effect is mediated to a large extent by electrostatic neutralization is bolstered by the fact that the endogenous polyamine spermine dose dependently inhibits FRET between the two proteins and prevents SOC influx (Calloway, unpublished data).

Complementary to these results, we observe formation of Orai1/CRACM1 patches at the plasma membrane following addition of D-sphingosine or DMS (Figure 7). STIM1 does not copatch under these conditions, suggesting that neutralization of the acidic residues by the sphingosine derivatives causes homo-oligomerization of Orai1/CRACM1, which could prevent its interaction with STIM1 by an effect on Orai1/CRACM1 structure. Importantly, SOC influx is not activated under these conditions (Figure 6A; data not shown).

Based on the primary structure of the recently identified interacting domains of STIM1 and Orai1/CRACM1 (Li *et al*., 2007, Muik *et al*., 2008), we hypothesized that association of the C-terminal polybasic region of STIM1 with the acidic C-terminal coiled-coil of Orai1/CRACM1 is important for the initiation of $I_{CRAC}$. Thus, Orai1/CRACM1 could be regulated in a manner similar to some TRP channels in which a C-terminal polybasic region regulates the activation of channel opening by electrostatic interaction with the plasma membrane (for review, see Rohacs 2006). As described above, this model also provides an explanation for inhibition of the interaction between STIM1 and Orai1/CRACM1 by D-sphingosine and DMS. To test whether the negatively charged residues on the putative C-terminal coiled-coil of Orai1/CRACM1 are involved in the interaction with STIM1, we mutated these residues to their neutral amide analogues. The results of our FRET measurements between STIM1-mRFP and AcGFP constructs of these Orai1/CRACM1 mutants provide clear evidence that these residues participate in the interaction between the two proteins (Figure 5B). The increase in FRET at long time points when only three residues are mutated could be the result of an altered stoichiometry between STIM1 molecules and Orai1/CRACM1 molecules in the interacting complex. This level of reduction in charge may require more Orai1/CRACM1 molecules to neutralize the charge on the polybasic region of STIM1. However, when all six acidic residues are mutated, the stimulated FRET is substantially decreased, potentially because the electrostatic driving force is largely eliminated. Residual FRET between STIM1-mRFP and AcGFP-Orai1/CRACM1ΔDE could be due to the presence of unmutated endogenous Orai1/CRACM1 in the clustered complex that interacts with clustered STIM1. Indeed, imaging of cells transfected with AcGFP-Orai1/CRACM1ΔDE reveals the formation of patches of this charge-neutralized protein in the absence of stimulation. The residual interaction between STIM1-mRFP and AcGFP-Orai1/CRACM1ΔDE detected by FRET could also involve other structural features of Orai1/CRACM1. Additionally, these mutations may affect other molecular interactions by Orai1/CRACM1, either with lipids or other proteins containing polybasic sequences.

As described above, the minimal effects of STIM1-mRFP and AcGFP-Orai1/CRACM1 expression on the strong SOCE response of endogenous STIM1and Orai1/CRACM1 provide evidence that our expression system does not significantly alter the homeostasis of RBL cells, but it limits our capability to observe changes in $Ca^{2+}$ influx caused by mutant Orai1/CRACM1 constructs. We therefore carried out these measurements in COS7 cells, which display very low levels of SOCE in untransfected cells (Figure 6B, solid circles). Consistent with previous results in these (Varnai *et al*., 2007) and other cell types (Soboloff *et al*., 2006), transient expression of STIM1-mRFP with AcGFP-Orai1/CRACM1 reconstituted robust SOCE (Figure 6B, open circles). However, when cells are transfected with STIM1-mRFP and AcGFP-Orai1/CRACM1ΔDE, this enhancement is dramatically reduced. These results confirm the functionality of the C-terminal acidic coiled-coil domain of Orai1/CRACM1, showing that these residues are necessary for both the interaction with STIM1 and the activation of $Ca^{2+}$ influx. Furthermore, these results show that the micron-scale clustering of AcGFP-Orai1/CRACM1ΔDE observed in the absence of STIM1-mRFP coclustering (Figure 7B) does not represent functional activation of CRAC.

The similarity of our findings with AcGFP-Orai1/CRACM1ΔDE and with D-sphingosine and DMS suggest a common mechanism for their effects and for the response to

thapsigargin stimulation: electrostatic neutralization of the C-terminal acidic residues of Orai1/CRACM1 by mutation, by interaction with positively charged D-sphingosine and DMS, and possibly by interaction with the polybasic region of STIM1 all induce the formation of micrometer-scale Orai1/CRACM1 clusters. Interestingly, only clustering induced by STIM1 activates $I_{CRAC}$, for reasons that are not yet clear.

In summary, our FRET measurements are consistent with our confocal imaging and provide a direct, quantitative measure of STIM1-Orai1/CRACM1 interactions that occur in molecular proximity in the plasma membrane of live cells. We observe time-dependent formation of STIM1–Orai1/CRACM1 complexes due to stimulation by thapsigargin or by antigen when $Ca^{2+}$ influx is prevented. However, under normal conditions of antigen stimulation, when refilling of $Ca^{2+}$ in ER stores is not prevented, STIM1-Orai1/CRACM1 interactions are highly regulated by store refilling. Furthermore, pharmacologic and mutational analyses provide evidence for an electrostatic mechanism for STIM1–Orai1/CRACM1 interactions and for the regulation of Orai1/CRACM1 oligomerization. These critical molecular interactions are dynamically regulated under physiological conditions of receptor-mediated $Ca^{2+}$ mobilization.

## ACKNOWLEDGMENTS

This work was supported by Chemistry/Biology Interface training grant (to N. C.) and by National Institutes of Health grant AI-022449.

## REFERENCES

Baba, Y. *et al*. (2006). Coupling of STIM1 to store-operated $Ca^{2+}$ entry through its constitutive and inducible movement in the endoplasmic reticulum. Proc. Natl. Acad. Sci. USA *103*, 16704–16709.

Baba, Y., Nishida, K., Fujii, Y., Hirano, T., Hikida, M., and Kurosaki, T. (2008). Essential function for the calcium sensor STIM1 in mast cell activation and anaphylactic responses. Nat. Immunol. *9*, 81–88.

Barr, V. A. *et al*. (2008). Dynamic movement of the calcium sensor STIM1 and the calcium channel orai1 in activated T-cells: puncta and distal caps. Mol. Biol. Cell *19*, 2802–2817.

Campbell, R. E., Tour, O., Palmer, A. E., Steinbach, P. A., Baird, G. S., Zacharias, G. S., and Tsien, R. Y. (2002). A monomeric red fluorescent protein. Proc. Natl. Acad. Sci. USA *99*, 7877–7882.

Das, R., Hammond, S., Holowka, D., and Baird, B. (2008) Real-time cross-correlation image analysis of early events in IgE receptor signaling. Biophys. J. *94*, 4996–5008.

Dellis, O., Dedos, S. G., Tovey, S. C., Taufiq-Ur-Rahman, Dubel, S. J., and Taylor, C. W. (2006). $Ca^{2+}$ entry through plasma membrane IP3 receptors. Science *313*, 229–233.

Erickson, M. G., Moon, D. L., and Yue, D. T. (2003). DsRed as a potential FRET partner with CFP and GFP. Biophys. J. *85*, 599–611.

Feske, S., Gwack, Y., Prakriya, M., Srikanth, S., Puppel, S. H., Tanasa, B., Hogan, P. G., Lewis, R. S., Daly, M., and Rao, A. (2006). A mutation in Orai1 causes immune deficiency by abrogating CRAC channel function. Nature *441*, 179–185.

Glitsch, M. D., and Parekh, A. B. (2000). $Ca^{2+}$ store dynamics determines the pattern of activation of the store-operated $Ca^{2+}$ current I(CRAC) in response to InsP3 in rat basophilic leukaemia cells. J. Physiol. *523*, 283–290.

Gosse, J. A., Wagenknecht-Wiesner, A., Holowka, D., and Baird, B. (2005). Transmembrane sequences are determinants of immunoreceptor signaling. J. Immunol. *175*, 2123–2131.

Grigoriev, I. *et al*. (2008). STIM1 is a MT-plus-end-tracking protein involved in remodeling of the ER. Curr. Biol. *18*, 177–182.

Guo, C., Holowka, D., and Baird, B. (1994). Fluorescence resonance energy transfer reveals interleukin (IL)-1-dependent aggregation of IL-1 type i receptors that correlates with receptor activation. J. Biol. Chem. *207*, 27562–27568.

Hoth, M., and Penner, R. (1992). Depletion of intracellular calcium stores activates a calcium current in mast cells. Nature *335*, 353–356.

Lewis, R. S., and Cahalan, M. D. (1989). Mitogen-induced oscillations of cytosolic $Ca^{2+}$ and transmembrane $Ca^{2+}$ current in human leukemic T cells. Cell Regul. *1*, 99–112.

Li, Z., Lu, J., Xu, P., Xie, X., Chen, L., and Xu, T. (2007). Mapping the interacting domains of STIM1 and Orai1 in $Ca^{2+}$ release-activated $Ca^{2+}$ channel activation. J. Biol. Chem. *282*, 29448–29456.

Liou, J., Kim, M. L., Heo, W. D., Jones, J. T., Myers, J. W., Ferrell, J. E., Jr., and Meyer, T. (2005). STIM is a $Ca^{2+}$ sensor essential for $Ca^{2+}$-store-depletion-triggered $Ca^{2+}$ influx. Curr. Biol. *15*, 1235–1241.

Liou, J., Fivaz, M., Inoue, T., and Meyer, T. (2007). Live-cell imaging reveals sequential oligomerization and local plasma membrane targeting of stromal interaction molecule 1 after $Ca^{2+}$ store depletion. Proc. Natl. Acad. Sci. USA *104*, 9301–9306.

Luik, R. M., Wu, M. M., Buchanan, J., and Lewis, R. S. (2006). The elementary unit of store-operated $Ca^{2+}$ entry: local activation of CRAC channels by STIM1 at ER-plasma membrane junctions. J. Cell Biol. *174*, 815–825.

Mathes, C., Fleig, A., and Penner, R. (1998). Calcium release-activated calcium current ($I_{CRAC}$) is a direct target for sphingosine. J. Biol. Chem. *273*, 25020–25030.

McCloskey, M. A., and Zhang, L. (2000). Potentiation of Fcε receptor I-activated $Ca^{2+}$ current ($I_{CRAC}$) by cholera toxin: possible mediation by ADP ribosylation factor. J. Cell Biol. *148*, 137–146.

Mercer, J. C., Dehaven, W. I., Smyth, J. T., Wedel, B., Boyles, R. R., Bird, G. S., and Putney, J. W. (2006). Large store-operated calcium selective currents due to co-expression of Orai1 or Orai2 with the intracellular calcium sensor, Stim1. J. Biol. Chem. *281*, 24979–24990.

Muik, M. *et al*. (2008). Dynamic coupling of the putative coiled-coil domain of ORAI1 with STIM1 mediates ORAI1 channel activation. J. Biol. Chem. *283*, 8014–8022.

Pierini, L. M., Harris, N. T., Holowka, D., and Baird, B. (1997). Evidence supporting a role for microfilaments in regulating the coupling between poorly dissociable IgE-FcεRI aggregates downstream signaling pathways. Biochemistry *36*, 7447–7456.

Peinelt, C., Lis, A., Beck, A., Fleig, A., and Penner, R. (2008). 2-Aminoethoxydiphenyl borate directly facilitates and indirectly inhibits STIM1-dependent gating of CRAC channels. J Physiol. *586*, 3061–3073.

Rohacs, T. (2006). Regulation of TRP channels by PIP2. Eur. J. Physiol. *453*, 753–762.

Roos, J. *et al*. (2005). STIM1, an essential and conserved component of store-operated $Ca^{2+}$ channel function. J. Cell Biol. *169*, 435–445.

Sato, T., Pallavi, P., Goebiewska, U., McLaughlin, S., and Smith, S. O. (2006). Structure of the membrane reconstituted transmembrane-juxtamembrane peptide EGFP (622–660) and its interaction with $Ca^{2+}$/calmodulin. Biochem. *45*, 12704–12714.

Smyth, J. T., DeHaven, W. I., Bird, G. S., and Putney, J. W. (2007). Role of the microtubule cytoskeleton in the function of the store-operated $Ca^{2+}$ channel activator STIM1. J. Cell Sci. 2007 *120*, 3762–3771.

Smyth, J. T., DeHaven, W. I., Bird, G. S., and Putney, J. W. (2008). $Ca^{2+}$-store-dependent and -independent reversal of Stim1 localization and function. J. Cell Sci. *121*, 762–767.

Soboloff, J., Spassova, M. A., Tang, X. D., Hewavitharana, T., Xu, W., and Gill, D. L. (2006). Orai1 and STIM reconstitute store-operated calcium channel function. J. Biol. Chem. *281*, 20661–20665.

van Rheenen, J., Langeslag, M., and Jalink, K. (2004). Correcting confocal acquisition to optimize imaging of fluorescence resonance energy transfer by sensitized emission. Biophys. J. *86*, 2517–2529.

Várnai, P., and Balla, T. (1998). Visualization of phosphoinositides that bind pleckstrin homology domains: calcium- and agonist-induced dynamic changes and relationship to myo-[3H]inositol-labeled phosphoinositide pools. J. Cell Biol. *19*, 501–510.

Varnai, P., Toth, B., Toth, D. J., Hunyady, L., and Balla, T. (2007). Visualization and manipulation of plasma membrane-endoplasmic reticulum contact sites indicates the presence of additional molecular components within the STIM1-Orai1 complex. J. Biol. Chem. *282*, 29678–29690.

Vig, M. *et al*. (2006a). CRACM1 multimers form the ion-selective pore of the CRAC channel. Curr. Biol. *16*, 2073–2079.

Vig, M. *et al*. (2006b). CRACM1 is a plasma membrane protein essential for store-operated $Ca^{2+}$ entry. Science *312*, 1220–1223.

Vig, M. *et al*. (2008). Defective mast cell effector functions in mice lacking the CRACM1 pore subunit of store-operated calcium release-activated calcium channels. Nat. Immunol. *9*, 89–96.

Wu, M. M., Buchanan, J., Luik, R. M., and Lewis, R. S. (2006). $Ca^{2+}$ store depletion causes STIM1 to accumulate in ER regions closely associated with the plasma membrane. J. Cell Biol. *174*, 803–813.

Wu, M., Holowka, D., Craighead, H. G., and Baird, B. (2004). Visualization of plasma membrane compartmentalization with patterned lipid bilayers. Proc. Natl. Acad. Sci. USA *101*, 13798–13803.

Yatomi, Y., Ruan, F., Megidish, T., Toyokuni, T., Hakomori, S., and Igarashi, Y. (1996). N,N-Dimethylsphingosine inhibition of sphingosine kinase and sphingosine 1-phosphate production in human platelets. Biochemistry *35*, 623–633.

Yeromin, A. V., Zhang, S. L., Jiang, W., Yu, Y., Safrina, O., and Cahalan, M. D. (2006). Molecular identification of the CRAC channel by altered ion selectivity in a mutant of Orai. Nature *443*, 226–229.

Zhang, L., and McCloskey, M. A. (1995). Immunoglobulin E receptor-activated calcium conductance in rat mast cells. J. Physiol. *483*, 59–66.